Phonon eigenvectors of chiral nanotubes

S. Reich and C. Thomsen
Institut für Festkörperphysik, Technische Universität Berlin, Hardenbergstrasse 36, 10623 Berlin, Germany

P. Ordejón
Institut de Ciència de Materials de Barcelona (CSIC), Campus de la U.A.B. E-08193 Bellaterra, Barcelona, Spain
(Received 20 June 2001; published 26 October 2001)

Although a commonly neglected fact, the physical properties of chiral carbon nanotubes may differ significantly from those of the usually considered, simpler achiral tubes. We show that the phonon eigenvectors, e.g., of the high-energy eigenmodes no longer fall into axial and circumferential modes as in armchair and zig-zag nanotubes. The atomic displacement may, instead, point in any tangential direction and even show an angular dependence of its direction around the circumference, as the results of *ab initio* calculations demonstrate.

DOI: 10.1103/PhysRevB.64.195416 PACS number(s): 78.30.Na, 63.22.+m

I. INTRODUCTION

The abundance of new phenomena found in single walled nanotubes comes from their one-dimensional nature and the multiple ways to roll up a graphene sheet to a tube. A nanotube is fully characterized by the vector along its circumference, the so-called chiral vector $\boldsymbol{c}=n_1\boldsymbol{a}_1+n_2\boldsymbol{a}_2$, where $\boldsymbol{a}_1$ and $\boldsymbol{a}_2$ form the elementary cell of graphene. While some properties such as, e.g., the elastic constants depend mostly on the diameter of a tube, others change drastically with the particular tube under consideration; the most prominent example for the latter being the electronic properties. Among the possible angles θ between $\boldsymbol{c}$ and $\boldsymbol{a}_1$ ($0°\leqslant\theta\leqslant 30°$) two are further distinguished: In the achiral tubes $\boldsymbol{c}$ is either parallel to $\boldsymbol{a}_1$, i.e., zig-zag tubes with $n_2=0$, or to $\boldsymbol{a}_1+\boldsymbol{a}_2$, i.e., armchair tubes with $n_1=n_2$. All other tubes are referred to as chiral.

Because of the crucial dependence of the nanotube properties on their structure, attempts to determine the diameters and chiral angles in real nanotube samples started soon after the discovery of this new carbon form. Whereas first reports seemed to indicate preferred chiralities around the armchair direction,[1] a homogeneous distribution of chiralities is now well established by a number of different techniques such as STM experiments,[2–4] electron diffraction,[5] and Raman scattering.[6] The homogeneous chirality distribution as found in experiment is contrasted by theoretical studies on a number of different topics which up to now have concentrated almost exclusively on the achiral tubes. For example, thermopower, quantum conductance and the effects of impurities and structural defects as well as the effect of oxygenation were studied with *ab initio* methods for achiral nanotubes. [7,8] Junctions between nanotubes were calculated for achiral (5,5) tubes,[9] and polarons were predicted with similar methods for various achiral nanotubes. [10] Using tight-binding molecular dynamics the coalescence of two adjacent (10,10) nanotubes was simulated.[11] Focussing on lattice dynamical properties we show that results on achiral nanotubes cannot simply be generalized. Instead, chiral tubes have to be treated explicitely and yield qualitatively and quantitatively different results from achiral ones.

Lattice dynamics studies beyond the simple zone folding approximation focus on armchair and to a less extent on zig-zag tubes with only a few exceptions.[12] This approach was found to be justified for the low-energy radial breathing mode, which is insensitive to the chiral angle, but it is certainly not satisfactory for a deeper understanding of the high-energy modes around 1600 cm^{-1} and their Raman spectra. Recently, polarized Raman measurements on aligned nanotubes and single tubes were published,[13,14] and compared to force constants and polarizability calculations for armchair tubes. The question arises whether the phonon eigenvectors for armchair tubes needed for this type of calculation are a good starting point for a comparison to Raman spectra from predominantly chiral tubes. This is in view of the fact that achiral in contrast to chiral tubes possess mirror planes, which fix the displacement either parallel or perpendicular to the nanotube axis.[15] In chiral tubes this imposes a too servere restriction on the phonon eigenvectors.

Here we report *ab initio* calculations of the vibrational properties of small chiral and achiral carbon nanotubes. In analyzing our results we concentrate on the eigenvectors and displacements. We find that the atomic displacements point in different directions in chiral nanotubes including the circumference and the *z* axis as well as the helical and the bond direction. The classification in LO and TO modes, which works well for achiral tubes, is thus meaningless in chiral nanotubes. Furthermore, we find that the degenerate *E* modes in chiral nanotubes even show a varying or ''wobbling'' displacement direction when going around the tube.

This paper is organized as follows. In Sec. II we discuss the eigenmodes in nanotubes and graphene from a symmetry point of view. While the eigenvectors in armchair or zig-zag nanotubes are completely determined by symmetry and some general assumptions on the strength of the in-plane and out-of-plane force constants, this is not the case for chiral tubes. Section III describes the details of the *ab initio* calculations. The calculated eigenvectors are discussed in Sec. IV. We present all Raman active high-energy modes of the calculated (8,4) and (9,3) chiral tube and introduce the displacement ellipses to specify the behavior of an eigenvector. We show how our results depend on the splitting of the axial and circumferential force constants and discuss our results in connection with Raman experiments on single walled carbon nanotubes. This work is summarized in Sec. V.

II. SYMMETRY

In this section we discuss general properties of the vibrations of carbon nanotubes which can be obtained from their symmetry. The phonon modes which received most attention in the literature are the Raman active high-energy vibrations and the radial breathing mode. We therefore concentrate on these particular phonons, but the concepts are straightforwardly generalized to any desired mode symmetry. Achiral tubes have eight Raman active modes $\Gamma^{\mathrm{R}}_{\mathrm{ac}}=2A_{1g}\oplus 2E_{1g}\oplus 4E_{2g}$ in armchair and $\Gamma^{\mathrm{R}}_{\mathrm{zz}}=2A_{1g}\oplus 3E_{1g}\oplus 3E_{2g}$ in zig-zag tubes.[15] The radial breathing mode always belongs to the A_{1g} representation, since it fully conserves the nanotube symmetry. The other eigenvectors can be found by group projector arguments: Achiral nanotubes are single orbit systems with the nontrivial stabilizer C_{1h}, i.e., one of their mirror planes transforms a given atom into itself.[16] Now consider an armchair tube for which we want to find the E_{1g} phonon eigenvectors. A circumferential (or radial) displacement is left invariant under σ_h, but then has to be multiplied by -1 for the projection onto the E_{1g} representation. The atomic displacement must thus be equal to its negative. Circumferential or radial eigenvectors are, therefore, never of E_{1g} symmetry in armchair nanotubes. The two E_{1g} modes have eigenvectors with an in-phase and out-of-phase displacement parallel to the *z* axis with two nodes around the circumference. Moreover, because of the different force constants for a tangential and radial displacement their eigenvectors are unlikely to mix. The atomic displacements in armchair and zig-zag tubes are thus expected to point either along the *z* axis, the circumference, or into the radial direction.

Another argumentation which is frequently found in the literature for the properties of the high-energy modes is the reference to graphene. Although it is a more hand-waving approach and not as compelling as the symmetry argumentations given so far, we want to introduce it here to point out the fundamental differences between achiral and chiral tubes. When looking at nanotubes as rolled up graphene sheets the circular boundary condition around the circumference quantize the corresponding wave vector k_θ. The Raman active high-energy vibrations may then be classified as LO_n and TO_n with respect to the confinement wave vector, where $2n=0,2,4$ gives the numbers of nodes around the circumference (note, though, that not all are Raman active because of the additional mirror or inversion symmetry).[17–19] The quantization direction of achiral nanotubes corresponds to high-symmetry direction of graphene, namely, Γ-*K*-*M* in armchair and Γ-*M* in zig-zag tubes. In these two *k* directions the graphene doubly degenerate E_{2g} optical phonon is split into a nondegenerate LO and TO mode belonging to two different representations. In chiral tubes, however, the confinement wave vector is along an arbitrary direction of the Brillouin zone. The only symmetry operations of graphene which leave k_θ invariant are the identity *E* and the horizontal mirror plane σ_h. There are now two in-plane nondegenerate optical modes with the same transformation properties. Since these modes are close in energy and of the same symmetry they are free to mix. The two phonon eigenvectors can neither be chosen arbitrarily within the plane (as for degenerate modes) nor are they fixed by symmetry as in the high-symmetry directions. The classification into LO and TO phonons is no longer valid *a priori*.

We now return to the tubes to see whether the full symmetry of chiral tubes provides more insight into the phonon eigenvectors. Among the two reasons given above for the classification into exclusively axial, circumferential, or radial displacement in achiral tubes, the second—a large difference between the radial and tangential force constants—holds for chiral tubes as well. The tangential displacement, however, is no longer determined by symmetry, because mirror planes are absent in chiral tubes. The atomic stabilizer is only the trivial *E* operation, no other symmetry transformation leaves any atom invariant. The total number of Raman active vibrations is 15 in chiral tubes, namely, $\Gamma^{R}_{\mathrm{ch}}=3A_1\oplus 6E_1\oplus 6E_2$. The horizontal rotation axes impose a small additional restriction on the chiral eigenmodes. The fully symmetric displacements must be in-phase for the radial, but out-of-phase for the two tangential A_1 modes. The E_m representations have $2m$ nodes around the circumference and both the in-phase and out-of-phase combination of the radial and the two tangential displacement directions. This yields a total of 6 modes for E_1 and E_2, respectively.

In this section we showed that while the phonon eigenvectors in achiral nanotubes are determined by the nanotube symmetry, no general conclusions can be obtained for chiral tubes. Although the curvature of the nanotube's wall introduces a softening of the circumferential force constants, the relative magnitude of the expected splitting is too small to predict the displacements. We therefore calculated the phonons in chiral and achiral nanotubes by first principles methods.

III. CALCULATIONS

Ab initio calculations were performed for (6,6) and (10,0) achiral and (8,4) and (9,3) chiral tubes using a numerical-atomic-orbital density-functional-theory method implemented in the SIESTA code.[20] We worked within the local-density approximation as parametrized by Perdew and Zunger.[21] Core electrons were replaced by nonlocal, norm-conserving pseudopotentials;[22] the valence electrons were described by a linear combination of numerical pseudo-atomic orbitals. We used a double-ζ, singly polarized basis set with cutoff radii for the *s* and *p* orbitals of 5.1 and 6.25 a.u., respectively.[23] Real space integrations were performed on a regular grid, corresponding to a plane wave cutoff around 240 Ry. The reader is referred to Ref. 24 for a successful application to nanotubes and other carbon systems[25,26] and to Ref. 20 for the general computational scheme.

After building the unit cell according to the idealized nanotube structure[15] we relaxed the single free-standing tube and infinite bundles of identical tubes by a conjugate gradient minimization. The nanotube radius *r*, the translational periodicity *a*, and the bundle lattice constant *b* we obtained are compared in Table I to the ideal cylindrical structure. The table also lists some other parameters as the chiral and helical angle and the screw axis generator. The agreement be-

TABLE I. Radius r, translational period a, bundle lattice constant b obtained in the *ab initio* calculations. The expected radius r_c and translational period a_c of an ideal clyindrical tube are given for comparison (obtained with the experimental graphene lattice constant of 2.461 Å). θ is the chiral angle and ϕ the angle between the helix and the circumference. The screw axis is denoted in the last column.

(n_1,n_2)	r (Å)	r_c (Å)	a (Å)	a_c (Å)	b (Å)	θ (°)	ϕ (°)	$(C_q^r\|an/q)$
(6,6)	4.11	4.07	2.466	2.461	11.36	30	30	$(C_{12}\|a/2)$
(8,4)	4.18	4.14	11.30	11.28	11.43	19.1	10.9	$(C_{56}^9\|a/14)$
(9,3)	4.27	4.24	15.44	15.39	11.49	13.9	5.2	$(C_{78}^{19}\|a/26)$
(10,0)	3.92	3.92	4.27	4.263	11.00	0	60	$(C_{20}\|a/2)$

tween our calculated r and a and the expected values is very good. The radii were found to be slightly hexagonally distorted ($<10^{-2}$) in the nanotube bundle, therefore in Table I we gave the mean values. The wall-to-wall distance is systematically lower than in graphite with the same basis set, 3.1 instead of 3.3 Å.

To obtain the dynamical matrix by a finite difference approach we calculated the Hellmann-Feynman forces for two displaced atoms.[25] The other forces were generated using the screw axis symmetry. Although nanotubes are single orbit systems and displacing one atom would be sufficient, we did not use the U axes in chiral and the mirror planes in achiral tubes.[15] The deviations from those symmetry operations in the eigenvectors measure the accuracy of our calculations. To further verify the symmetry based approach we performed a full calculation, i.e., displacing all atoms in the unit cell, for the (6,6) tube at zero and high pressure.[27] For the (10,0) and the two chiral tubes we used two different sets of atoms and compared the phonon frequencies and eigenvectors. For the achiral tubes the agreement was found to be excellent (within 3 cm^{-1}), somewhat larger in the chiral tubes (15 cm^{-1}) for the high-energy and the radial-breathing mode. The eigenvectors, however, were not affected in a fundamental way during the test calculations.

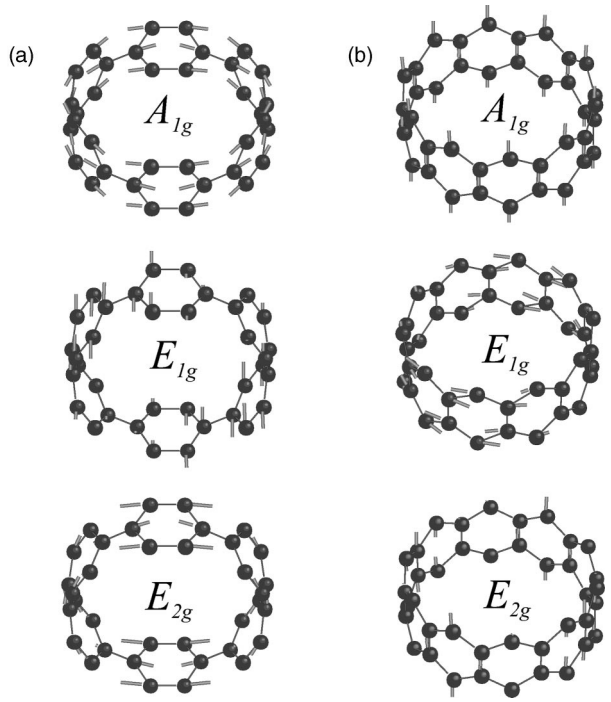

FIG. 1. Raman active A_{1g}, E_{1g}, and E_{2g} high-energy modes (a) of a (6,6) nanotubes and (b) of a (10,0) nanotube.

IV. PHONON EIGENVECTORS AND DISCUSSION

We first present the eigenvectors and frequencies of the two achiral nanotubes. The excellent agreement between our calculated and the symmetry imposed eigenvectors made us confident about our calculational procedure. Figure 1(a) and Table II show the A_{1g}, E_{1g}, and E_{2g} eigenvectors and frequencies of the high-energy modes in (6,6) and (b) in (10,0) nanotubes. All high-energy modes are found to be softened compared to graphene (1660 cm^{-1} in our calculations) in these fairly small tubes, which is in good agreement with previous *ab initio* calculations and experimental findings.[24,28] The softening appears to be a little overestimated for the A_1 circumferential mode, which is of A_{1u} symmetry in the (10,0) tube and at similar frequency (1550 cm^{-1}) as the A_{1g} in the armchair tube. Note that the ordering of the frequencies is non-trivially changed in the calculated tubes as compared to simple zone folding. Both confinement and curvature effects are, however, much stronger in the calculated tubes than in real samples with a typical mean radius ≈ 7 Å. In phonon calculations for achiral tubes of different diameter Dubay and Kresse found these effects to decrease rapidly with increasing diameter.[29] The calculated frequencies of the radial breathing mode in Table II are for achiral nanotube bundles. For single tubes we found a downshift of the frequency by 5–7 % as will be dicussed in detail elsewhere.

As can be seen in Fig. 1 the displacement patterns are in excellent agreement with the symmetry requirements. We found that the angle α between the atomic displacement and

TABLE II. Frequencies and displacement directions α for the Raman-active high-energy modes and the radial breathing mode in achiral nanotubes.

	(6,6)		(10,0)	
	ν (cm^{-1})	α (°)	ν (cm^{-1})	α (°)
RBM	285	0	289	2
A_{1g}	1545	0	1604	88
E_{1g}	1600	90	1606	2
E_{2g}	1629	0	1552	86

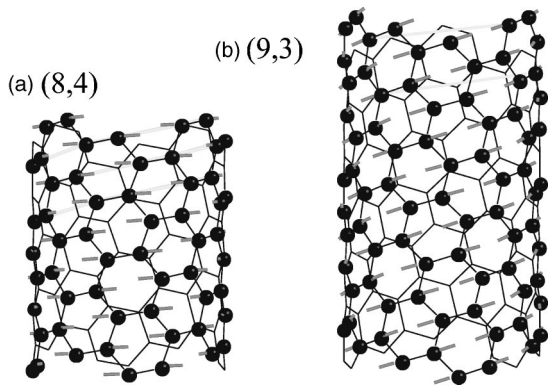

FIG. 2. (a) A_1 high-energy eigenvector of an (8,4) nanotube. The atomic displacement is parallel to the circumference. (b) A_1 high-energy eigenvector of a (9,3) tube. The displacement is parallel to the carbon-carbon bonds. The direction of the helix is indicated by the grey lines.

the circumference deviates by at most 5° from the circumferential $\alpha=0°$ or axial $\alpha=90°$ direction, showing the numerical accuracy of our calculation. We stress again that in the calculation of the force constants the mirror symmetries were not explicitly used.

In chiral nanotubes the atomic displacements are no longer, in general, along the cylindrical axes. In Fig. 2(a) we show an A_1 mode of an (8,4) tube and in (b) of a (9,3) tube. It can be seen that the displacement is along the circumference in the (8,4), but parallel to the bonds in the (9,3) nanotube. The smallest angle between the carbon-carbon bonds and the circumference in the (9,3) tube is $30°-\theta=16.1$, which coincides with the displacement direction as given in Table III. In the (8,4) tube we also found vibrations along the bond direction, but they were of B_1 and B_2 symmetry and hence not optically active.

We now take a look at the degenerate modes in chiral tubes. In Fig. 3 we show an E_1 eigenvector of an (8,4) nanotube. We successively rotated the nanotube by 32° to show the reader how the eigenvector evolves when going around the nanotube. As expected the magnitude of the atomic displacement (the length of the ticks) is modulated by a $\sin\varphi$ function. Contrary to what is generally expected, however, the direction of the displacement varies as well. Whereas the tick on the highlighted atom is perpendicular to one of the carbon-carbon bonds in the first picture, i.e., $\alpha\approx 40°$, they are almost parallel to the bonds with $\alpha\approx 10°$ in last two pictures; Table III lists the mean value $\alpha=33°$. For the E_2 eigenvector in the (8,4) tube no such variation is seen. The same sequence as in Fig. 3 is presented in Fig. 4 for the E_2 mode with a frequency of 1626 cm^{-1}. The atomic displacement is roughly parallel to the circumference in all four pictures.

TABLE III. Frequencies and average displacement directions for the high-energy and the radial breathing mode in chiral nanotubes.

	(8,4)		(9,3)	
	ν (cm^{-1})	α (°)	ν (cm^{-1})	α (°)
RBM	275	1	292	1
A_1	1670	−87	1627	16
A_1	1505	3	1519	−74
E_1	1610	33	1620	38
E_1	1591	−59	1607	−51
E_2	1626	−6	1638	7
E_2	1554	85	1587	−84

The angular dependence of the direction of the eigenvectors becomes more obvious when plotting the atomic displacement along the z axis versus the circumferential displacement (Fig. 5). The first two diagrams at the top in Fig. 5 corresponds to the A_1 high-energy modes in the (8,4) and (9,3) tube. For simplicity we considered only the displacement of the atoms belonging to the same graphene sublattice. Totally symmetric modes then show up as a single point in such a plot. The dashed lines point along the carbon-carbon bonds; the coincidence between the displacement and the bond direction in the (9,3) nanotube is obvious. A B symmetry mode (not shown) would be seen as two points in the z-xy displacement diagram, because the character of the screw axis generator is -1.[16] Open ellipses describe E symmetry eigenvectors with a varying or ''wobbling'' displacement direction. The principal axis of the ellipse gives the average angle of the eigenmode, i.e., α. The open ellipse with $\alpha\approx 33°$ of the (8,4) E_1 symmetry mode corresponds to the eigenvectors in Fig. 3. The degenerate eigenmode has the same ellipse. In general, the displacement of a degenerate eigenmode is obtained from a given eigenvector by a 90° rotation of the coordinate system around the z axis. The relationship between the axial and the circumferential displacement is thus the same for degenerate phonons. Two ellipses perpendicular two each other represent degenerate modes of the same symmetry but different frequencies. Correspondingly, the middle diagram of the (8,4) tube in Fig. 5 shows

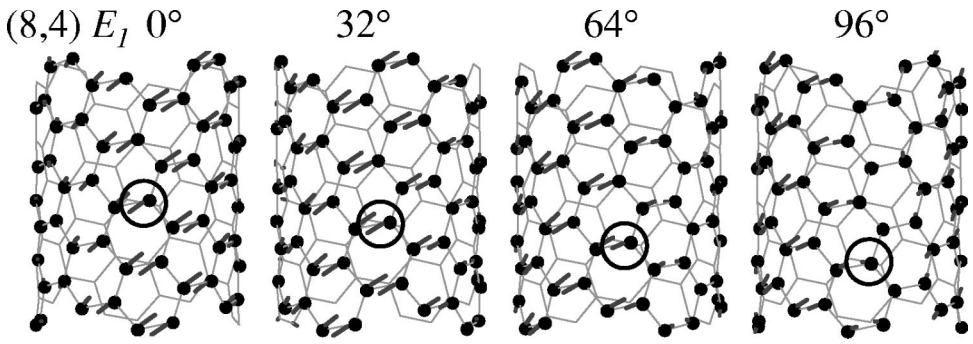

FIG. 3. Doubly degenerate E_1 eigenvector of an (8,4) tube with a frequency of 1610 cm^{-1}. The sequence shows the change in displacement when going around the tube in steps of 32°. The atoms which are highlighted by the small circles are connected by the screw symmetry of the tube.

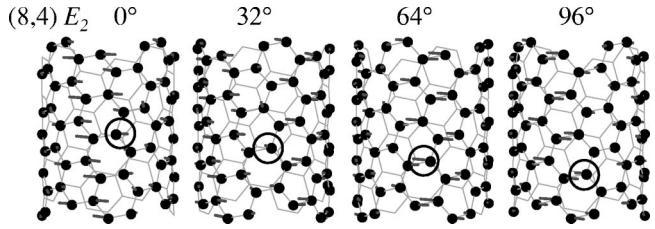

FIG. 4. E_2 high-energy mode of an (8,4) nanotube with a calculated frequency of 1626 cm^{-1}. The atomic displacement is along the circumference and, in contrast to Fig. 3, no wobbling is evident. The modulation of the displacement magnitude by a $\sin 2\varphi$ around the circumference is nicely seen when following the highlighted atom.

both the 1610 ($\alpha = 33°$) and the 1591 cm^{-1} ($-59°$) E_1 eigenvector.

In the middle panel to the right we depict the displacement for the E_1 modes in the (9,3) nanotube. The xy and the z displacment are again of similar magnitude, i.e., $\alpha \approx 40°$ and 50°, but they are now in phase and yield a constant direction of the atomic displacement around the tube. Two other examples of almost closed ellipses are the E_2 eigenmodes in both tubes (lowest panels in Fig. 5). Although the

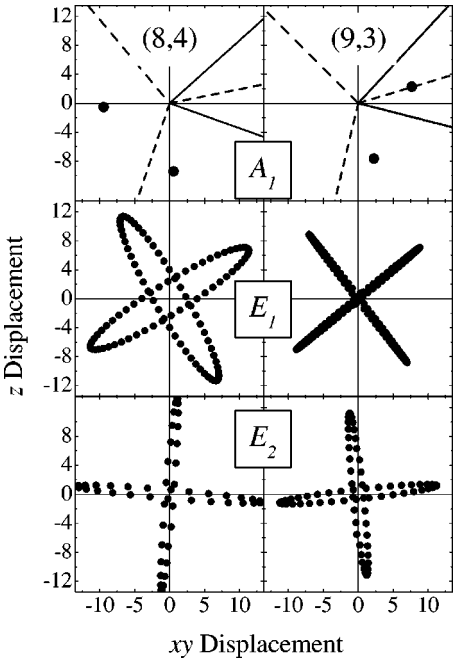

FIG. 5. z component of the displacement versus the xy circumferential component. Top: A_1 high-energy eigenvectors of an (8,4) tube (left) and a (9,3) tube (right). The dashed lines point in the direction of the carbon-carbon bonds, the full lines are parallel to $\boldsymbol{a}_1$ and $\boldsymbol{a}_2$. Middle: E_1 eigenvectors of the two chiral nanotubes. The atomic displacement direction is strongly varying in the (8,4) nanotube resulting in an open displacement ellipses. In the (9,3) nanotube the z and circumferential component are similar in magnitude but with an almost vanishing phase difference. Bottom: E_2 eigenvectors of the chiral tubes. The small z or xy component results in a closed ellipses almost parallel to the circumference or the nanotube axis.

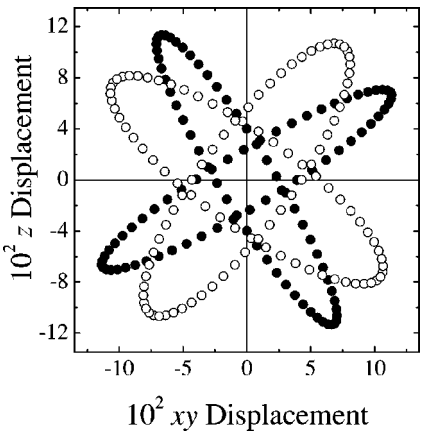

FIG. 6. Phonon eigenvectors with an reduced splitting between the axial and circumferential force constants. The eigenvector calculated by first principles methods is shown by the full dots [same as shown in Fig. 5 in the (8,4) E_1 diagram]. The open dots are the displacement ellipses for the E_1 high-energy eigenvectors after we slightly modified the force constants. The splitting between the two E_1 frequencies was reduced by 25%.

eigenvectors are in fact wobbling, the magnitude of the, e.g., the z displacement for the 1626 cm^{-1} E_2 (8,4) mode is very small. Therefore, the variation is not observable in the full eigenmode plot of Fig. 4.

The symmetry of a given phonon together with its displacement ellipse fully determine the phonon eigenvectors. The symmetry yields the $\sin m\varphi$ function of the axial and circumferential components, whereas the principle axes of the ellipses specify the relative magnitude and the phase shift between the two components.

In Sec. II we discussed that neither symmetry nor zone folding arguments are able to predict the phonon eigenvectors of chiral nanotubes. The absence of mirror planes and the low-symmetry confinement wave vectors in chiral tubes affect their vibrational properties in a fundamental manner. In particular, a classification of the high-energy modes into LO and TO vibrations is not applicable to chiral nanotubes. The mixed LO-TO character of the eigenvectors might have been expected from general physical considerations. The wobbling of the E symmetry modes—although fully consistent with symmetry—has never been suggested so far.

The crucial point for the wobbling and the mixed LO-TO character of the nondegenerate modes is the splitting in the axial and circumferential force constants introduced by confinement and curvature. Naturally, the question arises how the modes and the eigenvectors, in particular, will evolve if these two effects are reduced. To answer this question by first principles methods we would have to calculate a series of chiral nanotubes with the same chiral angle. The next candidates for the (8,4) and (9,3) series are a (12,8) and (12,6), which are beyond our computational capability. Nevertheless, to obtain general insight into the eigenmode behavior with a reduced splitting, we slightly changed the *ab initio* force constants to make them more similar. The relative splitting between, e.g., the two E_1 high-energy phonons of the (8,4) tube was reduced by 25%. In Fig. 6 we compare the former displacement ellipses (full dots) with the ellipses ob-

tained from the modified force constants (open dots). It is nicely seen that the two eigenvectors look more degenerate, i.e., the ellipses are more open. In the limit of identical force constants both eigenvectors will degenerate to a circle. The splitting of the force constants in real nanotubes will be less than in the small diameter nanotubes calculated in this work, but different from zero. The wobbling and the mixed LO-TO character of the high-energy phonons are thus even more dominant in real samples, because the wobbling is stronger for the modified force constants in Fig. 6 than for those calculated *ab initio*.

Finally, we comment on the phonon eigenvectors in connection with the wide range of Raman experiments in nanotubes. Recent experiments on isolated, aligned, and nonaligned nanotubes agree that the Raman spectrum of nanotubes is dominated by *zz* polarized scattering.[14,13,30,31] The relative contribution for this particular scattering geometry ranges from 60 to 100 % of the total intensity. Most likely, this strong anisotropy is due to the optical absorption probability, which seems to be much weaker for light polarized perpendicular than parallel to the nanotube axis. The details of the electron-phonon coupling have not been studied systematically.[32,10] In an *ab initio* calculation of polarons in zig zag nanotubes, however, Verissimo *et al.*[10] found that radial and axial deformations yield similar electron-phonon coupling. A circumferential or radial phonon eigenvector therefore not necessarily implies a weak resonant Raman cross section as it would be expected in nonresonant scattering.

Experimental support for our calculated phonon eigenvectors are Raman studies on single-walled nanotubes under high hydrostatic pressure.[33–35] The uniform shift of all high-energy modes under pressure in semiconducting nanotubes is contrasted by the highly anisotropic elastic properties of these material. We already pointed out that a mixed LO-TO character of the phonon eigenvectors in chiral nanotubes resolves this apparent discrepancy.[34] The differences in pressure slopes, which follow from the shear strain introduced by the anisotropic elastic constants, is not observable experimentally if the atomic displacements are pointing in arbitrary directions with respect to the nanotube axis.

V. SUMMARY

In summary, we showed by first-principle methods that results on physical properties on achiral nanotubes cannot simply be generalized to chiral tubes. We specifically calculated the vibrational eigenvectors of chiral nanotubes, which is the more commonly occurring type in any real sample. We displayed the A_1, E_1, and E_2 modes of (8,4) and (9,3) nanotubes and find that the eigenvectors no longer fall into axial and circumferential ones as was often assumed. Instead, they may have arbitrary angles α relative to the circumference. Furthermore, the doubly degenerate E_m eigenvectors show not only an angular dependence of the magnitude of the atomic displacement when going around the tube circumference, but a dependence of α as well. The displacement direction may ''wobble'' strongly around an average α if both the circumferential and axial components are large and have a finite phase difference. Our results show that many physical properties of carbon nanotubes may be considerably more complicated in real, chiral nanotubes than in the achiral ones which have served as model tubes so far.

ACKNOWLEDGMENTS

We acknowledge support from the Ministerio de Ciència y Technologia (Spain) and the DAAD (Germany) for a Spanish-German Research action (HA 1999-0118). P.O. acknowledges support from Fundación Ramón Areces (Spain), EU Project No. SATURN IST-1999-10593, and Spain-DGI Project No. BFM2000-1312-002-01. This work was supported by the Deutsche Forschungsgemeinschaft under Grant No. Th 662/8-1.

[1] A. Thess, R. Lee, P. Nikolaev, H. Dai, P. Petit, J. Robert, C. Xu, Y.H. Lee, S.G. Kim, A.G. Rinzler, D.T. Colbert, G.E. Scuseria, D. Tom'anek, J.H. Fischer, and R.E. Smalley, Science **273**, 483 (1996).

[2] T.W. Odom, J.L. Huang, P. Kim, and C.M. Lieber, Nature (London) **391**, 62 (1998).

[3] J.W.G. Wildöer, L.C. Venema, A.G. Rinzler, R.E. Smalley, and C. Dekker, Nature (London) **391**, 59 (1998).

[4] M. Ouyang, J.-L. Huang, C.L. Cheung, and C.M. Lieber, Science **292**, 702 (2001).

[5] L. Henrard, A. Loiseau, C. Journet, and P. Bernier, Eur. Phys. J. B **13**, 661 (2000).

[6] A. Jorio, R. Saito, J.H. Hafner, C.M. Lieber, M. Hunter, T. McClure, G. Dresselhaus, and M.S. Dresselhaus, Phys. Rev. Lett. **86**, 1118 (2001).

[7] K. Bradley, S.-H. Jhi, P.G. Collins, J. Hone, M.L. Cohen, S.G. Louie, and A. Zettl, Phys. Rev. Lett. **85**, 4361 (2000).

[8] H.J. Choi, J. Ihm, S.G. Louie, and M.L. Cohen, Phys. Rev. Lett. **84**, 2917 (2000).

[9] M.S. Fuhrer, J. Nygard, L. Shih, M. Forero, Y.-G. Yoon, M.S.C. Maoni, H.J. Choi, J. Ihm, S.G. Louie, A. Zettl, and P.L. McEuen, Science **288**, 494 (2000).

[10] M. Verissimo-Alves, R.B. Capaz, B. Koiller, E. Artacho, and H. Chacham, Phys. Rev. Lett. **86**, 3372 (2001).

[11] M. Terrones, H. Terrones, F. Banhart, J.-C. Charlier, and P.M. Ajayan, Science **288**, 1226 (2000).

[12] D. Kahn and J.P. Lu, Phys. Rev. B **60**, 6535 (1999).

[13] G.S. Duesberg, I. Loa, M. Burghard, K. Syassen, and S. Roth, Phys. Rev. Lett. **85**, 5436 (2000).

[14] A. Jorio, G. Dresselhaus, M.S. Dresselhaus, M. Souza, M.S.S. Dantas, M.A. Pimenta, A.M. Rao, R. Saito, C. Liu, and H.M. Cheng, Phys. Rev. Lett. **85**, 2617 (2000).

[15] M. Damnjanović, I. Milošević, T. Vuković, and R. Sredanović, Phys. Rev. B **60**, 2728 (1999).

[16] M. Damnjanović, T. Vuković, and I. Milošević, J. Phys. A **33**, 6561 (2000).

[17] A. Kasuya, Y. Sasaki, Y. Saito, K. Tohji, and Y. Nishina, Phys. Rev. Lett. **78**, 4434 (1997).

[18] A. Kasuya, M. Sugano, T. Maeda, Y. Saito, K. Tohji, H. Takahashi, Y. Sasaki, M. Fukushima, Y. Nishina, and C. Horie, Phys. Rev. B **57**, 4999 (1998).
[19] S.D.M. Brown, A. Jorio, P. Corio, M.S.D.G. Dresselhaus, R. Saito, and K. Kneipp, Phys. Rev. B **63**, 15 5414 (2001).
[20] D. Sanchez-Portal, P. Ordejón, E. Artacho, and J.M. Soler, Int. J. Chem. Quantum **65**, 453 (1997).
[21] J.P. Perdew and A. Zunger, Phys. Rev. B **23**, 5048 (1981).
[22] N. Troullier and J.L. Martins, Phys. Rev. B **43**, 1993 (1991).
[23] E. Artacho, D. Sánchez-Portal, P. Ordejón, A. García, and J. Soler, Phys. Status Solidi B **215**, 809 (1999).
[24] D. Sánchez-Portal, E. Artacho, J.M. Soler, A. Rubio, and P. Ordejón, Phys. Rev. B **59**, 12 678 (1999).
[25] P. Ordejón, E. Artacho, and J.M. Soler, Phys. Rev. B **53**, R10 441 (1996).
[26] E. Burgos, E. Halac, R. Weht, H. Bonadeo, E. Artacho, and P. Ordejón, Phys. Rev. Lett. **85**, 2328 (2000).
[27] S. Reich, C. Thomsen, and P. Ordejón (unpublished).
[28] C. Thomsen, Phys. Rev. B **61**, 4542 (2000).
[29] O. Dubay and G. Kresse, in *Electronic Properties of Novel Materials-Progress in Molecular Nanostructures*, *IWEPS Kirchberg*, edited by H. Kuzmany, J. Fink, M. Mehring, and S. Roth (AIP, Woodbury, 2001).
[30] H.H. Gommans, J.W. Alldredge, H. Tashiro, J. Park, J. Magnuson, and A.G. Rinzler, J. Appl. Phys. **88**, 2509 (2000).
[31] S. Reich, C. Thomsen, G.S. Duesberg, and S. Roth, Phys. Rev. B **63**, R041401 (2001).
[32] E. Richter and K.R. Subbaswamy, Phys. Rev. Lett. **79**, 2738 (1997).
[33] U.D. Venkateswaran, A.M. Rao, E. Richter, M. Menon, A. Rinzler, R.E. Smalley, and P.C. Eklund, Phys. Rev. B **59**, 10 928 (1999).
[34] S. Reich, H. Jantoljak, and C. Thomsen, Phys. Rev. B **61**, R13 389 (2000).
[35] P.V. Teredesai, A.K. Sood, S. Sharma, S. Karmakar, S.K. Sikka, A. Govindaraj, and C.N.R. Rao, Phys. Status Solidi B **B223**, 479 (2001).